Cement & Concrete Composites 30 (2008) 917–928

Contents lists available at ScienceDirect

Cement & Concrete Composites

journal homepage: www.elsevier.com/locate/cemconcomp

Comparative flexural behavior of four fiber reinforced cementitious composites

Dong joo Kim *, Antoine E. Naaman, Sherif El-Tawil

CEE Department, University of Michigan, 2350 Hayward, 2365 G.G. Brown Building, Ann Arbor, MI 48109-2125, United States

ARTICLE INFO

Article history:
Received 7 July 2008
Received in revised form 12 August 2008
Accepted 14 August 2008
Available online 29 August 2008

Keywords:
Deflection-hardening
Load capacity
Energy absorption capacity
Multiple cracking behavior
Fiber type
Fiber volume ratio
Toughness
Equivalent bond strength

ABSTRACT

This research investigates the flexural behavior of fiber reinforced cementitious composites (FRCC) with four different types of fibers and two volume fraction contents (0.4% and 1.2%) within a nominally identical mortar matrix (56 MPa compressive strength). The four fibers are high strength steel twisted (T-), high strength steel hooked (H-), high molecular weight polyethylene spectra (SP-), and PVA-fibers. The tests were carried out according to ASTM standards. The T-fiber specimens showed best performance in almost all aspects of behavior including load carrying capacity, energy absorption capacity and multiple cracking behavior, while the PVA-fiber specimens exhibited comparatively the worst performance in all aspects of response. The only category in which SP-fiber specimens outperformed T-fiber specimens was deflection capacity, where SP-specimens exhibited the highest deflection at maximum load. By comparing the test results to data from an additional test program involving the use of a higher strength mortar (84 MPa) with both H- and T-fibers, it is shown that, again, T-fibers perform significantly better than H-fibers in a higher strength matrix. The test results from both experimental programs were used to critique the new ASTM standard [C 1609/C 1609M-05], and a few suggestions were made for improving the applicability of the standard to deflection-hardening FRCCs.

1. Introduction

The addition of a relatively small quantity of short random fibers to a cementitious matrix is known to improve the mechanical response of the resulting product, commonly known as a fiber reinforced cementitious composite (FRCC). FRCCs have the potential of exhibiting higher strength and ductility in comparison to unreinforced mortar or concrete, which fail in tension immediately after the formation of a single crack. The performance of FRCC can be improved to the point where it exhibits a deflection-hardening response in bending accompanied by multiple cracks after initial cracking. In such a case, FRCC is known as deflection-hardening FRCC, or DHFRCC. The relationship between DHFRCC and strain-hardening FRCC in direct tension was discussed by Naaman [1]. He showed that, in order for the bending response to exhibit deflection-hardening, the average post-cracking strength in tension needs to be only about a third of the cracking strength. Thus a much smaller amount of fibers is required to obtain deflection-hardening response than to obtain strain-hardening behavior. Furthermore, Naaman [1] formulated an equation for the critical volume fraction of fibers to achieve deflection-hardening behavior. Recently, Soranakom and Mobasher [2] also discussed the correlation of tensile and flexural responses of FRCC and provided closed form equations to predict flexural behavior of FRCC based on its uniaxial tension and compression response. They also suggested that the tensile behavior of FRCC can be back-calculated from convenient flexural tests.

The performance of FRCC depends on many factors, such as fiber material properties (e.g., fiber strength, stiffness, and Poisson's ratio), fiber geometry (smooth, end hooked, crimped, twisted), fiber volume content, matrix properties (e.g., matrix strength, stiffness, Poisson's ratio), and interface properties (adhesion, frictional, and mechanical bond). Clearly, for a given matrix, the type and quantity of fibers are key parameters influencing the performance of FRCC and their cost. Everything else being equal, using a low fiber volume fraction, while still attaining strain-hardening or deflection-hardening response, is attractive from the cost point of view.

Although many researchers have conducted bending tests and reported the flexural response of FRCC, most used different sizes of specimen, matrix composition, and fiber and volume content in their experiments. Often, only one fiber type or material was considered and no attempt was made to compare performance with other fibers types or materials. Also, some researchers did not follow standard test procedures, e.g. as specified by ASTM. In addition, most of experimental studies that investigated the effect of fiber types were performed approximately a decade ago. Therefore, the types of fiber investigated in prior research are quite different from the high performance fibers used in this study. This situation, and the need to isolate the effect of fiber type on the flexural performance of FRCC, has motivated the experimental study reported in this paper, which focuses on the flexural performance

* Corresponding author. Tel.: +1 734 936 2405; fax: +1 734 764 4292.
E-mail address: kdjoo@umich.edu (D.j. Kim).

0958-9465/$ - see front matter © 2008 Elsevier Ltd. All rights reserved.
doi:10.1016/j.cemconcomp.2008.08.002

of FRCC involving four high performance fibers within a nominally identical mortar matrix (56 MPa compressive strength).

The main objective of this research is to investigate the influence of fiber type and fiber volume content on the bending response of four FRCCs. Testing and analysis of results were carried out according to ASTM standard C 1609/C 1609M-05 [3]. The research is geared towards mixtures showing deflection-hardening behavior with low to moderate fiber contents, here, 0.4% and 1.2% by volume. To gain further insight into the effect of matrix strength, the results of this research are compared to test results from a related program involving the use of a higher strength matrix (84 MPa compressive strength). The test results lead to some suggestions to improve current standard ASTM C 1609.

2. Bending behavior of FRCC beams

Much research on the bending behavior of FRCC has been carried out over the past four decades in US and elsewhere. Soroushian and Bayasi [4] investigated the effect of fiber type on the general performance of fiber reinforced concrete. They used different types of steel fibers, including straight-round, crimped-round, crimped-rectangular, hooked-single, and hooked-collated fibers with 2% fiber volume content. They reported that the overall workability was independent of fiber type except for crimped fiber. They also noted that hooked fibers showed better performance than straight and crimped fibers.

Gopalaratnam et al. [5] pointed out the importance of accurate deflection measurement in estimating toughness and other parameters describing flexural behavior of FRCC. They also noted that the effect of fiber type, fiber volume fraction and specimen size could be discerned from toughness measures. Balaguru et al. [6] investigated the flexural toughness of FRCC with deformed steel fibers using the procedure for deflection measurement suggested by Gopalaratnam et al. [5]. They investigated three types of fibers: hooked-end, corrugated, and end deformed steel fibers. In computing toughness, they used the I5 and I10 indices defined according to the ASTM C 1018 [7] procedure. Their results indicated that the toughness indices did not reflect the variations observed in the load–deflection curves. They also noted that, of the three types of fibers investigated, hooked-end fibers were the most effective in improving toughness.

Banthia and Trottier [8] pointed out several difficulties in both ASTM C 1018 and JSCE SF-4 methods for FRCC toughness characterization and suggested an alternative technique. For the former method (ASTM C 1018), they discussed the difficulty of measuring deflection correctly, and accurately identifying the first cracking point. For the latter (JSCE SF-4), they showed that the flexural toughness (FT) factor depends upon the geometry of the specimen and noted that the end-point used in the computation, at span-over-150, is arbitrary and actually much greater than the deflection at serviceability.

Several points necessary to estimate the performance of deflection-hardening FRCC were discussed by Naaman [1]. In addition to the toughness index for describing the toughness of FRCC, he recommended using the average post-cracking strength or surface energy as additional parameters. He also defined ductility as the ratio of total energy consumed up to a certain point to the elastic energy and mentioned that the scale effect and testing procedure could influence multiple cracking in strain-hardening or deflection-hardening FRCC.

Chandrangsu and Naaman [9] compared the performance of three different fibers, twisted (Torex), spectra, and PVA-fiber, in both tensile and bending response using two different specimen sizes. The length of the fibers was 30 mm for Torex fibers, 38 mm for spectra fibers, and 12 mm for PVA-fiber. The smaller bending specimens had a 75 mm × 12.5 mm thin rectangular section with 225 mm span length, while the larger size bending specimens had a 100 mm × 100 mm square section with 300 mm span length. The twisted (Torex) fibers generated best performance in both tensile and bending test among the three fibers considered. In addition, a strong size effect was noticed especially in the bending test, in terms of strength and deflection. The smaller bending specimens showed 80% higher modulus of rupture, and 500% higher deflection (actual displacement not normalized) at maximum load compared with the larger specimens.

3. Parameters describing flexural behavior of FRCC

The bending behavior of FRCC can generally be classified as either deflection-softening or deflection-hardening, as shown by curves (a) and (b), respectively, in Fig. 1 [10]. FRCC showing deflection-hardening behavior generates a higher load carrying capacity after first cracking compared with normal concrete or deflection-softening FRCC. In this research, the first cracking point is defined as the point where nonlinearity in the load–deflection curve becomes evident. This point is termed limit of proportionality (LOP) according to the previous ASTM standard C 1018-97 [7]. The new ASTM standard C 1609/C 1609M-05 [3] uses the first peak point, defined as a point where the slope is zero, which is inappropriate for use with materials exhibiting deflection-hardening with multiple micro cracks. In other words, it is hard to pinpoint the first peak strength as required by ASTM standard C 1609/C 1609M-05 [3] if the bending behavior of the material shows stable deflection-hardening as shown in the upper curves of Fig. 1. Therefore, LOP is used in this work instead of first peak strength. The load value at LOP is termed P_{LOP} and the corresponding deflection value is δ_{LOP} in Fig. 1. The stress obtained when the first cracking load is inserted into Eq. (1) is defined as the first-crack strength, f_{LOP}. The energy equivalent to the area under the load–deflection curve up to LOP is defined as first-crack toughness $Tough_{LOP}$. This definition is consistent with the ASTM standard definition for toughness at various points of the load–deflection curve, as explained farther below. From ASTM C 1609/C 1609M-05 [3], the stress at LOP is obtained from

$$f_{LOP} = P_{LOP} \cdot \frac{L}{bh^2}, \tag{1}$$

where L is the span length, b is the width of specimen, and h is the height of specimen.

The modulus of rupture (MOR) is defined as the point where softening starts to occur after point LOP as shown in Fig. 1. Besides the LOP and MOR points, six other points are defined as follows:

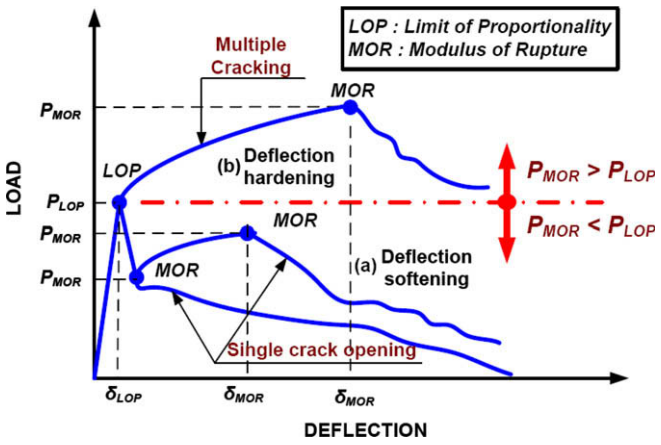

Fig. 1. Typical load–deflection response curves of FRCC.

Table 1
Matrix of test program

Matrix	Fiber volume contents (%)	T-fiber	H-fiber	SP-fiber	P-fiber
Mortar	1.2	T12	H12	SP12	PVA12
	0.4	T04	H04	SP04	PVA04

Table 2
Composition of matrix mixtures by weight ratio and compressive strength

Cement[a]	Fly ash[d]	Sand[b] (Flint)	Super-plasticizer	VMA[c]	Water	f'_c, ksi (MPa)
1.00	0.15	1.00	0.009	0.006	0.35	8.1 (55.9)

[a] ASTM Type 3 Portland Cement.
[b] ASTM 50-70.
[c] Viscosity modifying agent.
[d] Type C.

Table 3
Properties of fibers

Fiber type	Diameter (mm)	Length (mm)	Density (g/cc)	Tensile strength, ksi (MPa)	Elastic modulus, ksi (GPa)
High strength steel Torex	0.012 (0.3)[a]	1.18 (30)	7.9	320 (2206)[b]	29,000 (200)
High strength steel hooked	0.015 (0.38)	1.18 (30)	7.9	304 (2100)	29,000 (200)
Spectra	0.0015 (0.038)	1.50 (38)	0.97	374 (2585)	16,960 (117)
PVA #13	0.0078 (0.2)	0.472 (12)	1.3	140 (1000)	4203 (29)

[a] Equivalent diameter.
[b] Tensile strength of the fiber after twisting.

$d5$: point at a deflection of 3.0 times δ_{LOP},
$d10$: point at a deflection of 5.5 times δ_{LOP},
$d20$: point at a deflection of 10.5 times δ_{LOP},
$L/600$: a net deflection equal to 1/600 of the span,
$L/150$: a net deflection equal to 1/150 of the span, and
$L/100$: a net deflection equal to 1/100 of the span,

where the *L/600, L/150,* and $L/100$ deflections correspond to 0.5 mm (0.02 in.), 2 mm (0.08 in.), and 3 mm (0.12 in.), respectively, for the specimen clear span of 300 mm (12 in.).

The ASTM Standard C 1609 recommends use of the $L/600$ and $L/150$ points. However, it was found in this investigation that these points are insufficient to fully differentiate behavior between different fibers, and one additional point was added, namely $L/100$. For all tested specimens, load, stress, and toughness (energy) quantities were computed from the test results for the six points listed above in addition to LOP and MOR. To facilitate referring to various quantifies, the prefixes P, f, δ, Tough are used to designate load, stress, displacement, and toughness associated with a specific point (as was done for LOP).

4. Experimental program

The matrix used for all specimens had a nominal compressive strength of 8.1 ksi (56 MPa). The fibers used were high strength steel twisted (T-), high strength steel hooked (H-), high molecular weight polyethylene spectra (SP-), and PVA-fibers and were applied in two fiber volume contents (0.4% and 1.2%) leading to eight series of bending specimens designated as shown in Table 1. Two specimens per series were prepared for T- and H-fiber series, while three specimens per series were used in the SP- and PVA-fiber series. Fewer specimens were used in the T- and H-fiber series because prior tests showed very consistent results. Table 2 provides

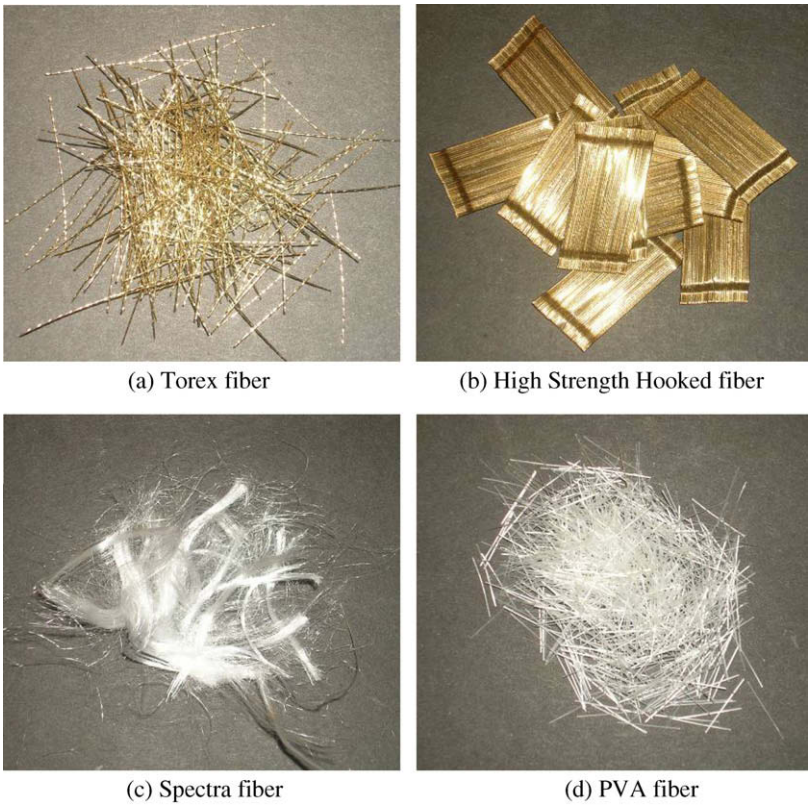

Fig. 2. Pictures of fibers.

the mortar mixture composition for the matrix used and its average compressive strength. Fiber properties are given in Table 3, and Fig. 2 shows pictures of the T-, H-, SP-, and PVA-fibers used. A servo-hydraulic testing machine (MTS 810) running in displacement control was used to conduct the bending tests. To reduce testing time, the rate of net displacement increase was taken as 0.25 mm/min (0.01 in./min), which is somewhat higher than the rate of 0.10 mm/min (0.004 in./min) recommended in ASTM C 1609/C 1609M-05 [3].

4.1. Materials and specimen preparation

A Hobart type laboratory mixer was used to prepare the mix. Cement, fly-ash, and sand were first dry-mixed for about 2 min. Water, mixed with super-plasticizer and a viscosity modifying agent (VMA), was then added gradually and mixed for another 5–10 min. The VMA was added into the matrix mixture to increase viscosity, prevent fiber sinking, and improve fiber distribution, as noted by Ozyurt et al. [11]. When the mortar started to show adequate flowability and viscosity, both of which are necessary for good workability and uniform fiber distribution, fibers were dispersed carefully by hand into the mortar mixture. The cementitious mixture with fibers was then carefully placed in a mold by using a wide scoop and vibrated using a high frequency vibrating table. Sufficient time of vibration was provided to guarantee suitable consolidation and to prevent fiber protrusion from the finished surface. During mixing and placing of the fresh mixture, no steel fiber gravitation was observed and uniform fiber distribution was apparent. Specimen casts were covered with plastic sheets and stored at room temperature for 24 h prior to demolding. The specimens were then placed in a water tank for an additional 4 weeks. All specimens were tested in a dry condition at the age of 32 days, which allowed 4 days for drying in a laboratory environment. Two to three layers of polyurethane were sprayed on the surface of the specimens after drying to facilitate crack detection.

4.2. Test setup and procedure

The geometry of the test specimen and the test setup are shown in Fig. 3. The size of beam used is 100 × 100 × 350 mm (4 × 4 × 14 in.) in accordance with ASTM standard C 1609/C 1609M-05. The clear span is 300 mm (12 in.). Before testing, specimens are rotated 90° from their casting position to reduce the effects of casting direction on the test results. A special test frame was used to measure the center deflection as shown in Fig. 3. This frame made it possible to eliminate extraneous deformations such as deformation from seating or twisting of the specimen. The frame was located at mid-depth of the specimen using four screws at points A and B as shown in Fig. 3. Only two of the screws provided a fixed restraint against displacement, while the two other allowed horizontal displacement. Deflection was measured from an LVDT attached to the frame and the load signal was measured from a load cell directly attached to the bottom of the cross head. A 5 Hz data acquisition frequency was used to record static load and deflection signals.

4.3. Test results and general discussion

The flexural response of all test series is illustrated by the load–deflection curves in Fig. 4. Each load–deflection curve in the figure is averaged from two or three specimens as previously discussed. Detailed information about the test results are also documented in Tables 4 and 5, which give averaged values of the parameters characterizing the flexural behavior of FRCC at the eight points previously defined.

Two different scales are used for the load axes of the graphs in Fig. 4a and b, since a significant difference in load carrying capacity was noted for the different fiber volume contents studied. As illustrated in Fig. 4a, even though the test series demonstrated a wide range of performance, all test series with 1.2% fiber volume content exhibited deflection-hardening behavior. Of the series with 0.4% fiber volume content (Fig. 4b), three series (T04, H04, and SP04) generated deflection-hardening behavior while only PVA04 resulted in deflection-softening response. The deflection-hardening series (T04, H04, and SP04) exhibited similar load–deflection responses, unlike the test series with 1.2% fiber volume content, which exhibited different load–deflection characteristics.

In comparing the flexural performance according to the type of fiber, the load–deflection curves in Fig. 4a and b illustrate that T-fiber reinforced specimens produced the highest load carrying capacity and MOR compared with other series. However, SP-fiber specimens showed the best deflection capacity at MOR. The MOR for T-fiber specimens was almost three times higher than that observed for specimens with PVA-fiber at both fiber volume contents.

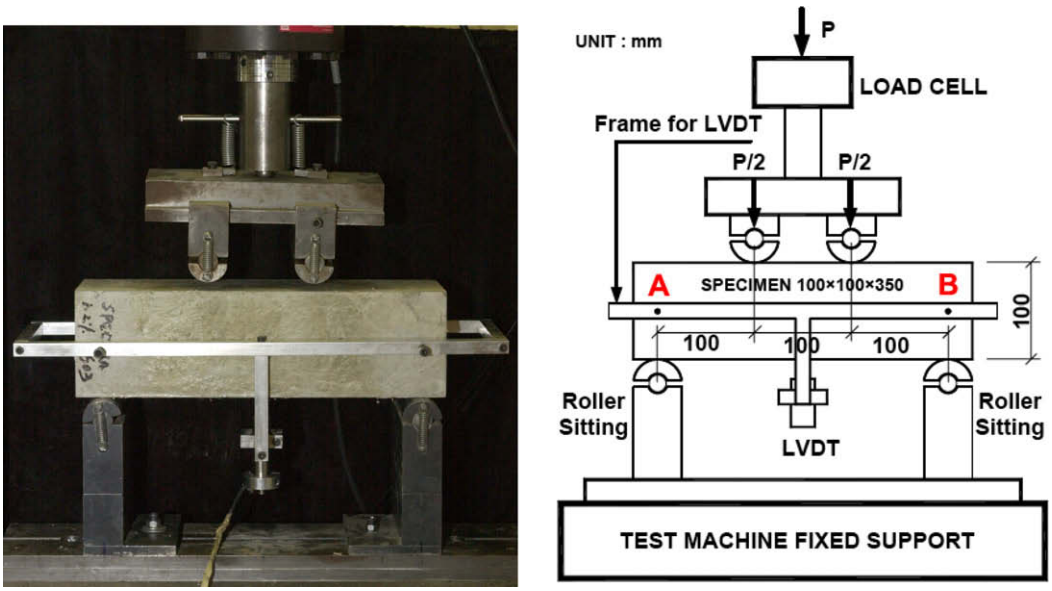

Fig. 3. Test specimen and setup.

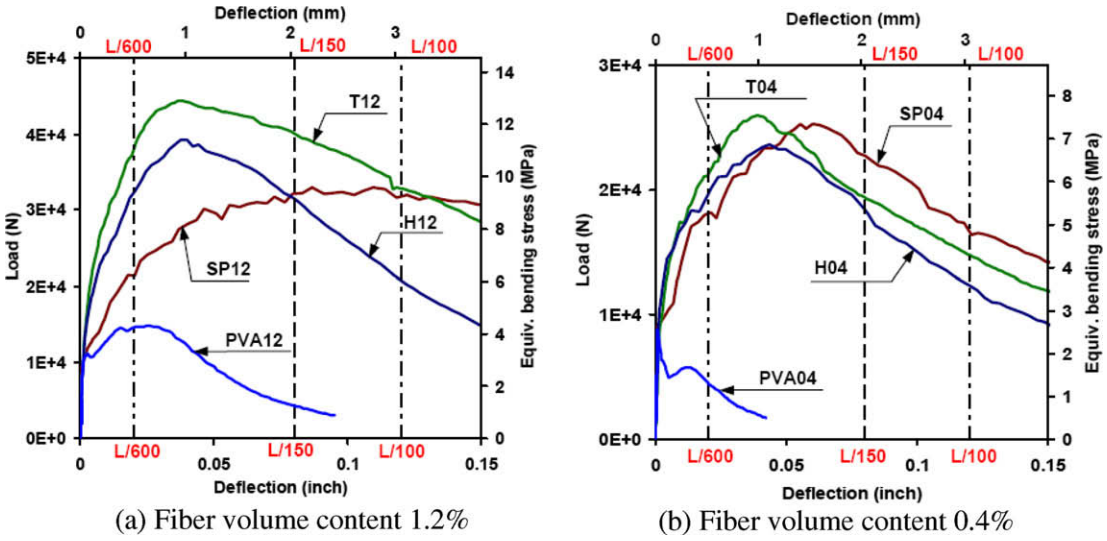

Fig. 4. Bending test results with medium strength matrix.

Table 4
Average response quantities for flexural behavior of FRCC (V_f = 1.2%)

		Unit	T12	H12	SP12	PVA12
LOP	P_{LOP}	N	9005	8927	9487	10,756
	f_{LOP}	MPa	2.62	2.60	2.76	3.13
	δ_{LOP}	mm	2.4E−2	2.3E−2	2.4E−2	2.6E−2
	$Tough_{LOP}$	N m	0.116	0.112	0.078	0.147
*d*5	P_{d5}	N	17,886	16,054	11,410	10,814
	f_{d5}	MPa	5.20	4.67	3.32	3.15
	δ_{d5}	mm	7.2E−2	7.0E−2	7.3E−2	7.9E−2
	$Tough_{d5}$	N m	0.789	0.726	0.613	0.747
*d*10	P_{d10}	N	23,084	20,420	14,489	11,433
	f_{d10}	MPa	6.71	5.94	4.21	3.33
	δ_{d10}	mm	1.3E−1	1.3E−1	1.3E−1	1.5E−1
	$Tough_{d10}$	N m	2.051	1.804	1.405	1.481
*d*20	P_{d20}	N	29,566	25,070	18,325	13,185
	f_{d20}	MPa	8.60	7.29	5.33	3.83
	δ_{d20}	mm	2.5E−1	2.4E−1	2.6E−1	2.8E−1
	$Tough_{d20}$	N m	5.226	4.466	3.415	3.114
L/600	$P_{L/600}$	N	38,014	33,157	23,553	15,880
	$f_{L/600}$	MPa	11.06	9.64	6.85	4.62
	$\delta_{L/600}$	mm	0.5	0.5	0.5	0.5
	$Tough_{L/600}$	N m	13.823	12.171	8.838	6.479
MOR	P_{MOR}	N	44,982	39,843	34,483	16,212
	f_{MOR}	MPa	13.08	11.59	10.03	4.72
	δ_{MOR}	mm	1.2	0.9	3.05	0.6
	$Tough_{MOR}$	N m	44.117	28.453	90.679	7.384
L/150	$P_{L/150}$	N	40,214	31,522	31,736	4379
	$f_{L/150}$	MPa	11.70	9.17	9.23	1.27
	$\delta_{L/150}$	mm	2.0	2.0	2.0	2.0
	$Tough_{L/150}$	N m	78.889	69.328	54.402	21.316
L/100	$P_{L/100}$	N	33,517	20,771	34,053	0
	$f_{L/100}$	MPa	9.75	6.04	9.90	0
	$\delta_{L/100}$	mm	3.0	3.0	3.0	3.0
	$Tough_{L/100}$	N m	116.608	94.015	88.424	22.755

Table 5
Average response quantities for flexural behavior of FRCC (V_f = 0.4%)

		Unit	T04	H04	SP04	PVA04
LOP	P_{LOP}	N	7823	8788	7714	9408
	f_{LOP}	MPa	2.28	2.56	2.24	2.74
	δ_{LOP}	mm	3.2E−2	2.6E−2	1.9E−2	2.5E−2
	$Tough_{LOP}$	N m	0.129	0.128	0.077	0.123
*d*5	P_{d5}	N	12576	12982	9944	7141
	f_{d5}	MPa	3.66	3.78	2.89	2.08
	δ_{d5}	mm	9.6E−2	7.7E−2	5.7E−2	7.4E−2
	$Tough_{d5}$	N m	0.779	0.708	0.442	0.531
*d*10	P_{d10}	N	16130	14530	11080	4962
	f_{d10}	MPa	4.69	4.23	3.22	1.44
	δ_{d10}	mm	1.8E−1	1.4E−1	1.0E−1	1.4E−1
	$Tough_{d10}$	N m	1.922	1.615	0.930	0.898
*d*20	P_{d20}	N	18799	17502	13337	5539
	f_{d20}	MPa	5.47	5.09	3.88	1.61
	δ_{d20}	mm	3.4E−1	2.7E−1	2.0E−1	2.6E−1
	$Tough_{d20}$	N m	4.673	3.689	2.107	1.552
L/600	$P_{L/600}$	N	21628	19612	19843	4748
	$f_{L/600}$	MPa	6.29	5.70	5.77	1.38
	$\delta_{L/600}$	mm	0.5	0.5	0.5	0.5
	$Tough_{L/600}$	N m	8.247	8.063	7.243	2.927
MOR	P_{MOR}	N	26151	23970	27130	5935
	f_{MOR}	MPa	7.61	6.97	7.89	1.73
	δ_{MOR}	mm	1.0	1.2	1.6	0.3
	$Tough_{MOR}$	N m	21.399	22.922	35.239	2.086
L/150	$P_{L/150}$	N	19017	18705	24113	0
	$f_{L/150}$	MPa	5.53	5.44	7.01	0.00
	$\delta_{L/150}$	mm	2.0	2.0	2.0	2.0
	$Tough_{L/150}$	N m	43.433	41.057	43.798	4.360
L/100	$P_{L/100}$	N	14227	12195	16271	0
	$f_{L/100}$	MPa	4.14	3.55	4.73	0.00
	$\delta_{L/100}$	mm	3.0	3.0	3.0	2.0
	$Tough_{L/100}$	N m	60.179	56.365	63.920	4.360

The cracking behavior (crack width, spacing, number, shape) of FRCC specimens is investigated because it is one of the main parameters characterizing the performance of each fiber type. It is clear from Fig. 5 that there is a large variation in the cracking response based on fiber type and volume content. Indeed, all test series showed multiple cracks except series PVA04, which responded in a deflection-softening manner as previously indicated. Generally, specimens with higher fiber volume content exhibited more cracks than specimens with lower fiber volume content. In addition, specimens with T- and SP-fibers exhibit the highest number of cracks. Specimens with PVA-fibers produced only 2–3 cracks in specimens with 1.2% fiber volume content and only one major crack (with immediate localization) in specimens with 0.4% fiber volume content. Details of the multiple cracking responses of the T12 and SP12 series are shown in Fig. 5i and j.

4.4. Load carrying capacity (equivalent bending stress)

The effect of fiber type on the equivalent bending stress is illustrated in Fig. 6. Eight equivalent bending stress values were calculated from the bending loads at different deflection points using Eq. (1). The deflection points were selected from the

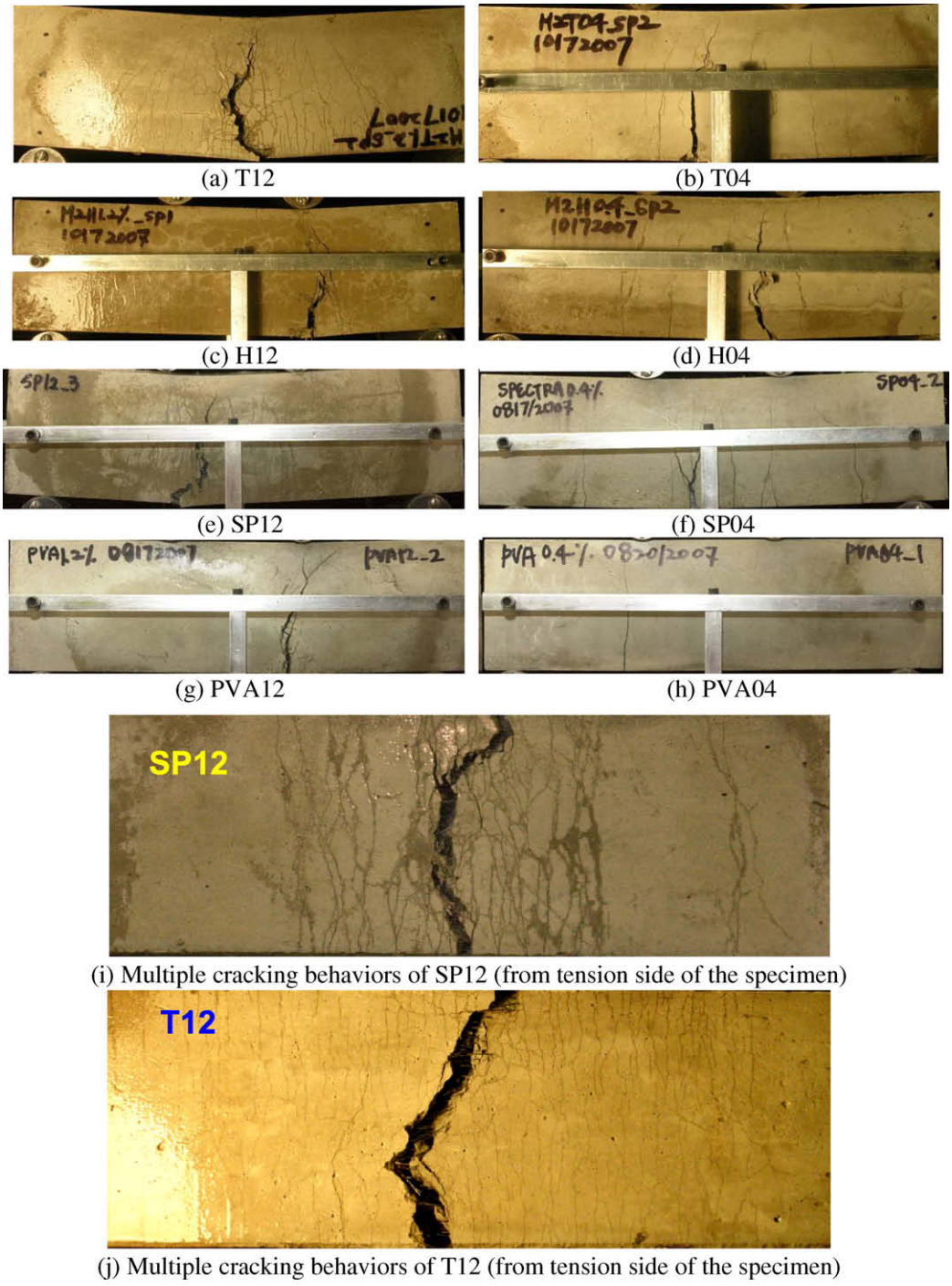

Fig. 5. Cracking behavior of FRCC under bending.

load–deflection curves of the test series as previously explained. Fig. 6a and c describes the development of flexural load resistance in the ascending range of the load–deflection curves, while Fig. 6b and d illustrates the effect of fiber type on the different softening tendencies of load resistance in the descending range of the load–deflection curves.

Fig. 6a shows the equivalent bending stress in the test series with 1.2% fiber volume content up to and including the $L/600$ deflection point, while Fig. 6b shows the equivalent bending stress at MOR, $L/150$ and $L/100$. This same arrangement is used for series with 0.4% fiber volume content in Fig. 6c and d.

In Fig. 6a, the effect of the types of fiber on the equivalent bond strength at LOP is not apparent for all series with 1.2% fiber volume content. For example, f_{LOP}, is 2.62 MPa for T12, 2.60 MPa for H12, 2.76 MPa for SP12, and 3.13 MPa for PVA12. A more noticeable effect of fiber type is observed as the deflection increases following LOP. This result shows that the effect of fiber reinforcement is activated primarily after LOP through fiber bridging and that the bridging forces are highly dependent upon the type of fiber. The equivalent elastic bending strength values at other deflection points of interest, $d5$, $d10$, $d20$, and $L/600$ are documented in Table 4 and plotted in Fig. 6a; for example, $f_{L/600}$ is 11.06 MPa for T12,

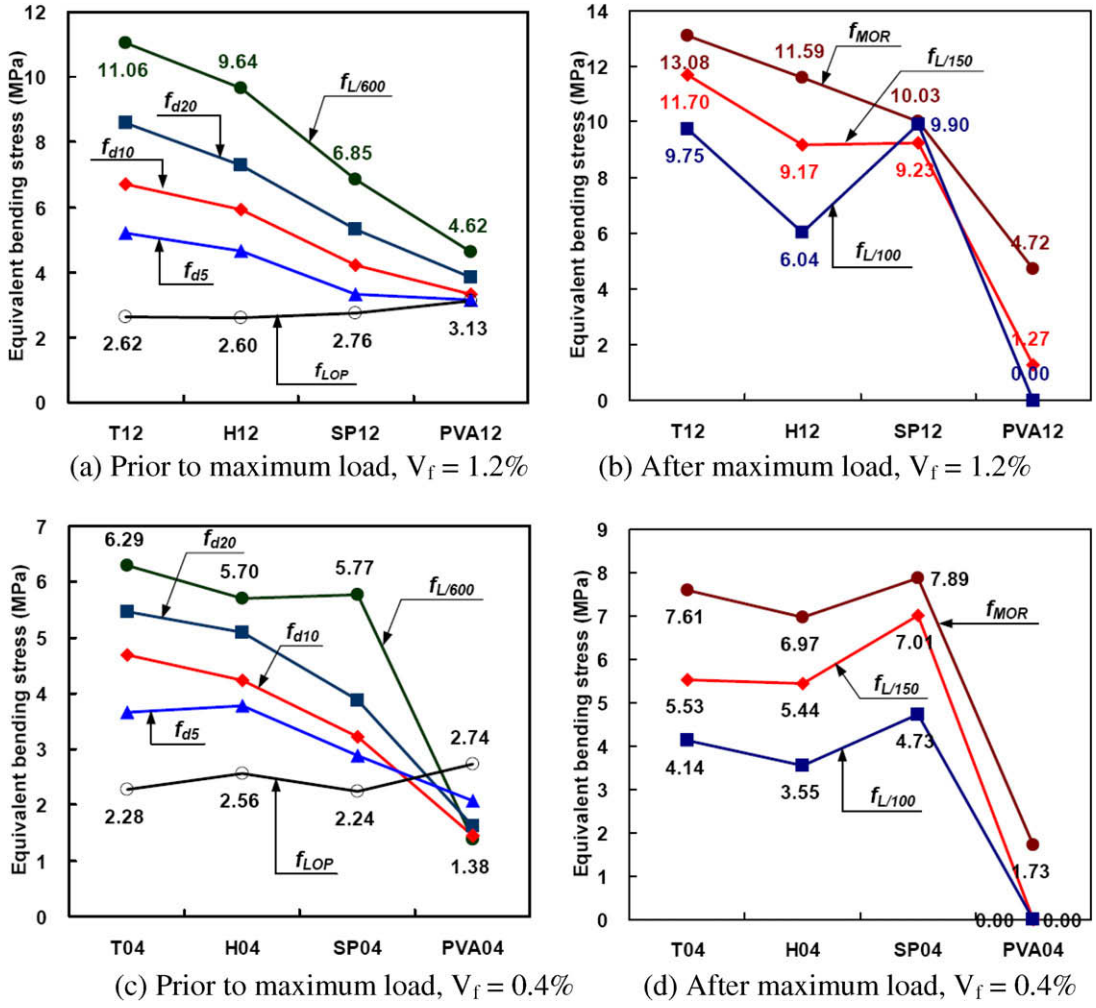

Fig. 6. Effect of fiber type on equivalent bending stress.

9.64 MPa for H12, 6.85 MPa for SP12, and 4.62 MPa for PVA12. The same trend is also evident at MOR as shown in Fig. 6b. Clearly, in terms of strength at MOR, T-fibers perform the best while PVA-fibers perform the worst. The ratio of their MOR is approximately three at 1.2% fiber content, and four at 0.4% fiber content.

Deflection points $L/150$ and $L/100$ were primarily intended to sample response in the softening range. While softening at these deformation levels is achieved in most series, Series SP12 is an exception and is still in the hardening range at $L/150$ and $L/100$. Displacement at maximum load, δ_{MOR}, for SP12 is 3.05 mm (Table 4), which is higher than $\delta_{L/100}$ (=3 mm), reflecting the extreme ductility of this series. On the contrary, Series PVA12 did not show any residual strength at $L/100$ in Fig. 6b since PVA12 loses most of its load carrying capacity at $L/150$. Breakage of PVA-fibers was clearly observed at the major crack opening in PVA-series, while, in contrast, series with other fiber types exhibited fiber pullout.

The variation of the equivalent bending stress in the test series with 0.4% fiber volume contents is illustrated in Fig. 6c and d. As for the case of lower fiber content, little variation of f_{LOP} with fiber type was observed, although f_{LOP} stresses were somewhat lower than those with higher fiber volume content. As previously indicated, and as shown in Figs. 4b and 6c, only PVA04 underwent deflection-softening behavior, while all other series exhibited deflection-hardening response in spite of the low fiber volume content. The equivalent bending stress values at other pertinent deflection points in the ascending range of the load–deflection curve are also shown in Fig. 6c and Table 5.

Unlike series with a higher fiber volume content, Series T04, H04, and SP04 had similar values of f_{MOR}. For example, as shown in Fig. 6d, f_{MOR} is 7.61 MPa, 6.97 MPa, 7.89 MPa, respectively. Figs. 4b and 6d show that the softening branches for series T04, H04, and S04 are also quite similar. In contrast, f_{MOR} (=1.73 MPa) is much lower in PVA04, which softens much more quickly than its three other counterparts, as previously indicated.

4.5. Energy absorption capacity (toughness)

There is need for high energy absorbing materials that will mitigate the hazards for structures subjected to dynamic loads, such as seismic, impact, and blast. Thus comparing energy absorption capacity provides useful information for such applications. The effect of fiber type on energy absorption capacity is illustrated in Fig. 7 using toughness values, defined as the area up to a certain deflection under the load–deflection curve. Fig. 7a shows the effect of fiber type on the toughness of the test series with 1.2% fiber volume content up to and including the $L/600$ point (essentially along the ascending branch of the curve), while Fig. 7b illustrates the toughness as a function of fiber type at MOR, $L/150$, and $L/100$ deflection points on the descending branch of the curve except for Series SP12. The same arrangement is used for the series with 0.4% fiber volume content in Fig. 7c and d.

As shown in Fig. 7a, toughness values of different fiber reinforced specimens at LOP are almost same in all series with 1.2% fibers. The same observation is true for deflection points $d5$ and $d10$.

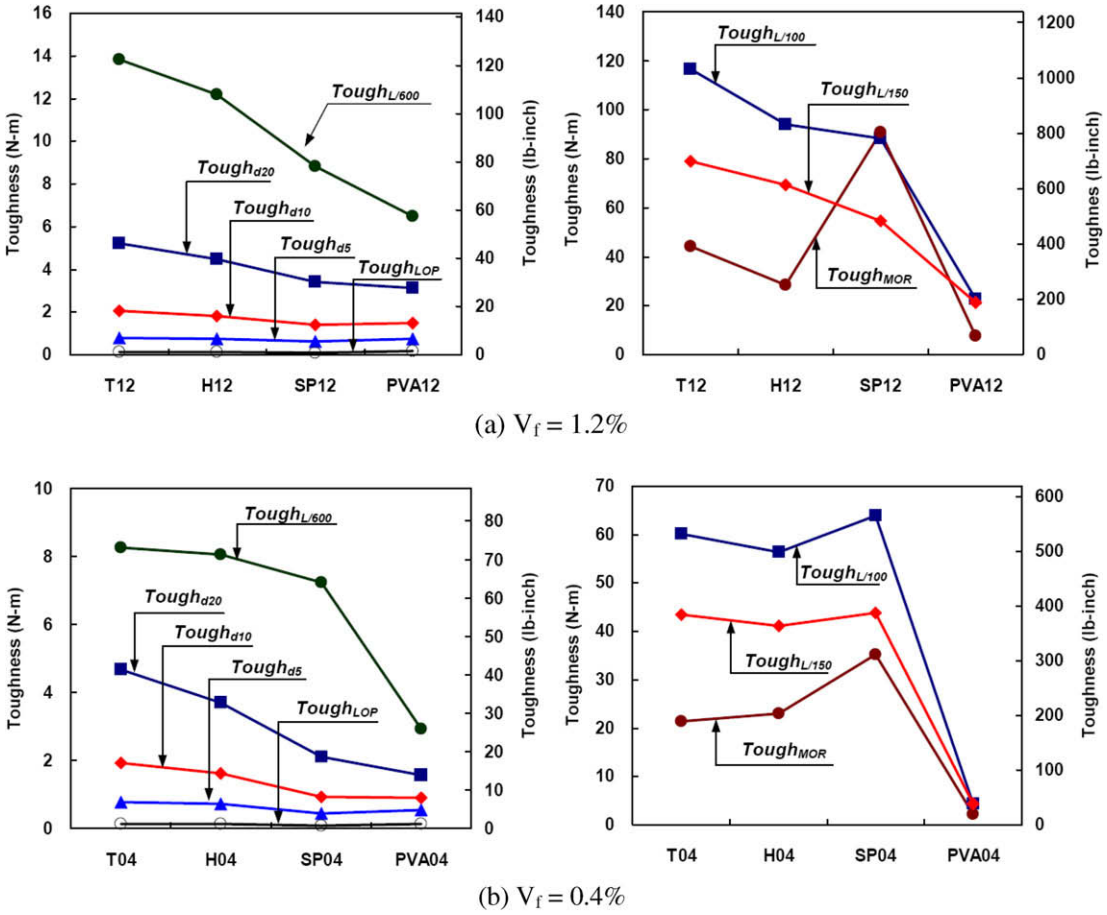

Fig. 7. Effect of fiber type on toughness.

However, noticeable differences between specimens with different types of fiber start to occur at $d20$ and beyond because the load resistance increases. For example, at point $L/600$ in ascending range of load–deflection curve, toughness values are 13.823 N m for T12, 12.171 N m for H12, 8.838 N m for SP12, and 6.479 N m for PVA12, respectively. Thus, for toughness values up to $L/600$, specimens with T-fibers provide the toughest response, while PVA-fiber provides the lowest toughness, with H-fiber and SP-fiber specimens in between. As shown in Fig. 7b and Table 4, the same general trend can be observed at $L/150$ and $L/100$. However, the situation is different at MOR, where specimens with SP-fibers outperform T-fiber specimens and absorb significantly more energy. This is, of course, attributed to the extreme ductility of Series SP12 in the hardening range.

The variation of toughness in specimens T04, SP04, and H04 is lower than for their counterparts with 1.2% fibers. In addition, different trends were observed. For example, H-fiber specimens slightly outperform specimens with T-fibers at MOR. In addition, specimens with SP-fibers continue to outperform T-fiber specimens at $L/150$ and $L/100$, which did not occur at 1.2% volume fraction.

4.6. Deflection characteristics

Structural ductility is a function of deflection capacity, which is the motivation for the study in this section. Deflection, δ_{LOP}, at LOP is clearly not dependent on the type of fiber or fiber volume content as shown in Fig. 8 and Tables 4 and 5. In contrast, the deflection at maximum load, δ_{MOR}, is highly dependent upon the type of fiber and volume content. For example, as shown in Fig. 8a, δ_{MOR} is 1.2 mm for T12, 0.9 mm for H12, 3.05 mm for SP12, and 0.6 mm for PVA12. Here, SP12 outperforms all other series, again because of its extended deflection-hardening range. The best performance for the low fiber content also occurs in specimens with SP-fibers, where δ_{MOR} is 1.0 mm for T04, 1.2 mm for H04, 1.6 mm for SP04, and 0.3 mm for PVA04, as shown in Fig. 8b. In general, it is obvious that the deflection capacity is strongly influenced by fiber content only in the specimens with SP-fibers. In other words, the deflection of specimens at maximum resistance with T-, H-, and PVA-fibers exhibited lower dependence on fiber content than specimens with SP-fibers.

4.7. Strength ratio and toughness ratio

To provide a general idea about the comparative performance of fibers, the strength and toughness of all test series were normalized by the values of PVA-fiber reinforced series, since the strength and toughness of PVA-fiber reinforced specimens were the lowest. This was not done for the lower volume fraction because PVA04 produced deflection-softening behavior. Strength ratio and toughness ratio are illustrated in Fig. 9.

The three equivalent bending stresses for the 1.2% series, $f_{L/600}$, f_{MOR}, and $f_{L/150}$, were divided by the equivalent bending stress of PVA-fiber reinforced specimen. As shown in Fig. 9a, T12 generates an equivalent bending stress at $\delta_{L/600}$ and δ_{MOR} of 2.39 and 2.77 times that of PVA12, respectively. When the deflection reaches $\delta_{L/150}$, T12 showed a strength capacity that is 9.18 times that of PVA12.

The toughness ratio of various series compared to that with PVA-fibers at 1.2% fiber content is illustrated in Fig. 9b. Toughness ratios at $\delta_{L/600}$ and $\delta_{L/150}$ deflections are in following order; T-fi-

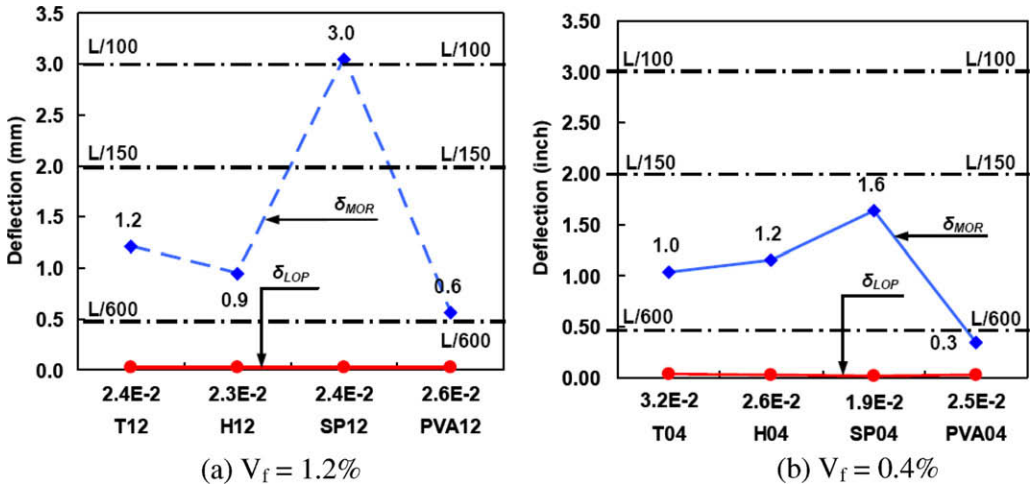

Fig. 8. Effect of fiber type on deflection δ_{LOP} and δ_{MOR}.

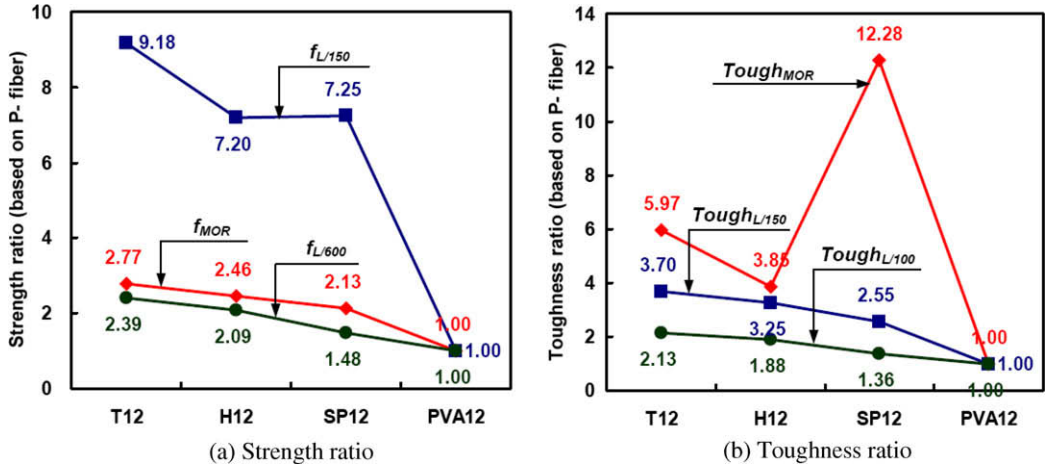

Fig. 9. Strength and toughness ratio based on PVA-fiber.

bers > H-fibers > SP-fibers > PVA-fibers. T12 produced the highest toughness ratio, i.e. 3.70 and 2.13, at deflections $\delta_{L/600}$ and $\delta_{L/150}$, respectively. In comparing toughness, $Tough_{MOR}$ at maximum resistance, SP12 showed the highest toughness ratio due to its high deflection capacity δ_{MOR}.

4.8. Comparative performance of twisted (T-) and hooked (H-) fiber in high strength matrix

As an additional experimental investigation [12], the performance of FRCC in bending with the same high strength steel T- and H-fibers in a high strength mortar matrix was evaluated. The compressive strength of the matrix was 84 MPa. Two fiber volume contents (1.0% and 2.0%) were used and three specimens were tested in each series. The test series are identified as T10-H, T20-H, H10-H, H20-H for the two types of fiber and the two fiber contents, respectively, where the appended '-H' at the end of each designation refers to the high strength matrix. Investigating the effect of matrix strength on the same key composite strength and toughness values described above (Figs. 6 and 7) with a lower strength matrix provides further insight into the behavior of FRCCs.

Average load–deflection curves and photos of typical cracking behavior for the high strength matrix series are shown in Fig. 10a. As observed in the other tests discussed above, T-fiber specimens showed both higher load carrying capacity and energy absorption capacity than H-fiber specimens, and generated significantly better cracking response.

Load carrying capacity and energy absorption capacity for the high strength matrix series are compared in Fig. 10b and c. As shown in Fig. 10b, f_{MOR} is 29.42 MPa for T20-H, 22.21 MPa for H20-H, 16.78 MPa for T10-H, and 6.58 MPa for H10-H. It is observed from Fig. 10b that T-fibers are more effective than H-fibers in the presence of a higher strength matrix. It also appears, when comparing Fig. 10b and c with Figs. 6 and 7, that generally speaking a higher strength matrix leads to improved FRCC performance. For example, f_{MOR} is 13.08 MPa for T12 with the lower strength matrix (56 MPa) and 16.78 MPa for T10-H with the higher strength matrix (84 MPa). Similarly, the toughness at $L/100$ for the T10-H (high strength matrix) is higher than the corresponding toughness of T12 for the lower strength matrix, yet it has a smaller volume fraction of fibers.

Overall, it is observed that increasing the matrix compressive strength increases the performance of T-fibers significantly more than that of H-fibers. That is, T-fibers take better advantage of the higher strength matrix.

4.9. Comments on current ASTM standard C 1609/C 1609M-05

The ASTM Standard C 1609/C 1609M-05 [3] replaces its predecessor ASTM Standard C 1018-97 [6]. While the new standard is

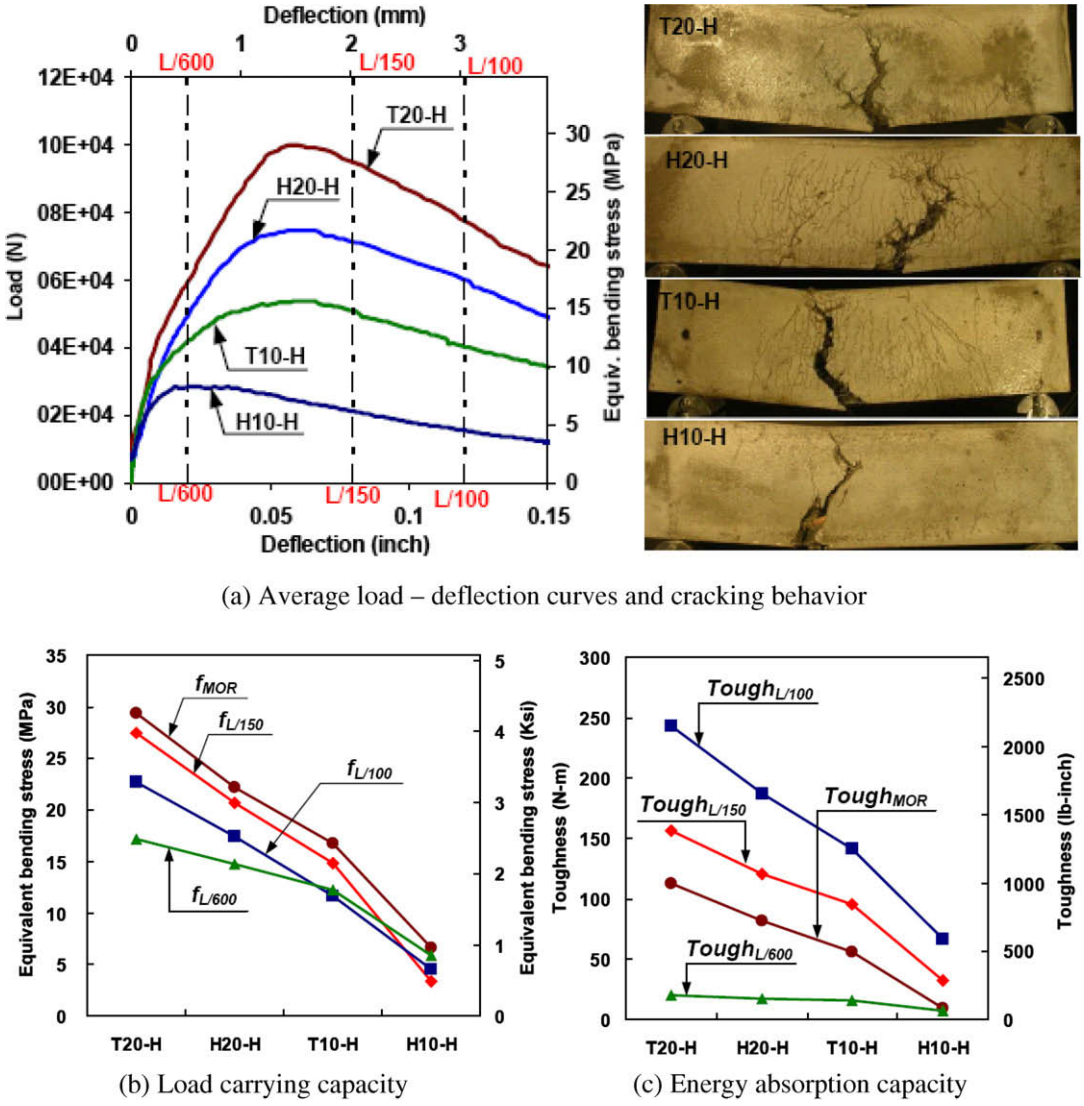

Fig. 10. Bending test results with high strength matrix.

certainly an improvement over the older one in some respects, there are a number of difficulties that arise when the new standard is applied to deflection-hardening composites.

The C 1609 Standard recommends estimating toughness as the "energy equivalent to the area under load–deflection curve up to a net deflection of 1/150 of the span". For deflection-hardening response, especially in situations involving large deformation in the deflection-hardening range (in excess of $L/150$), such as observed here in the SP series, the situation becomes more complicated because the computed toughness may not then truly represent the energy absorption capacity of the material. It is therefore suggested that the computations of toughness be extended to $L/100$ and even $L/50$ if the case justifies it. More research is needed to determine the end deflection point, such as $L/150$, $L/100$, and $L/50$.

Another difficulty with the C 1609 Standard pertains to the definition of LOP, which is defined as the first point on the load–deflection curve where the slope is zero. Clearly, deflection-softening FRCC will exhibit such response. On the other hand, deflection-hardening FRCC may not show such a load drop and may not possess a point on their load–deflection curve where a zero slope is meaningful in the sense suggested by the C 1609 Standard. For example, Fig. 11, where the load–deflection curves are not averages but typical examples from each test series. In Fig. 11a, PVA12 clearly shows an LOP point in accordance with C 1609, however, such a point with zero slope cannot be meaningfully detected on the load–deflection curves of T12, H12, and SP12. Even at low fiber volume content of 0.4%, T04 and H04 show no clear load drop, whereas SP04 and PVA04 both show a load drop with definable LOP. Together, these observations imply that a first peak point cannot always be found in the initial portion of a load–deflection curve if the specimen shows stable deflection-hardening response, i.e. without a sudden load drop after LOP. With this in mind, LOP is more generally applicable than the first peak point in describing the flexural behavior of deflection-hardening FRCC. Fig. 11c illustrates that although there is no point where the slope is zero in the initial part of the load–deflection curve of T12, by magnifying the scale of the deflection axis, a possible LOP point (that is, deviation from linearity but without zero slope) can be found.

5. Conclusions

This research investigated the flexural behavior of FRCC employing four different types of fibers with two volume fraction

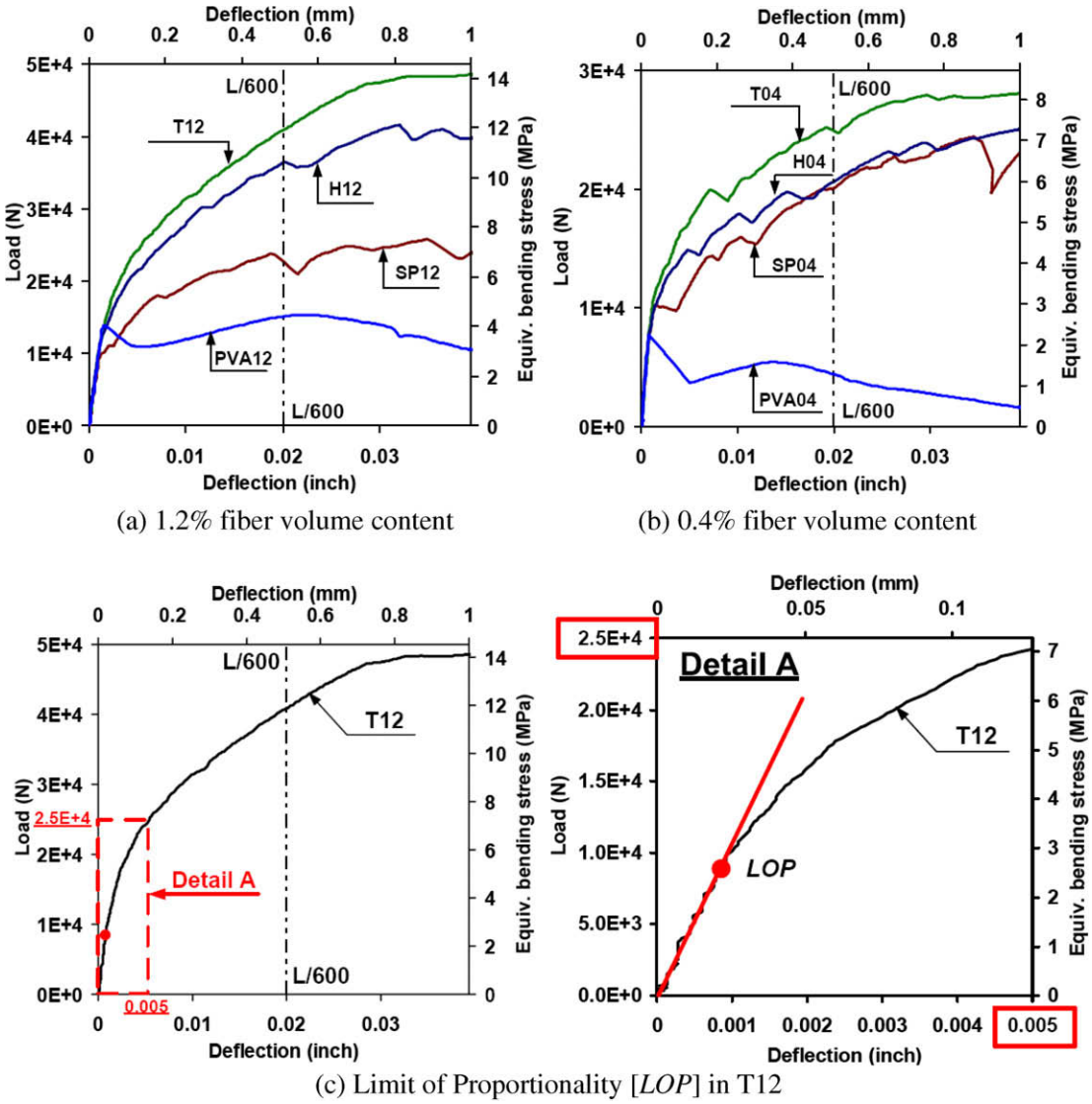

(a) 1.2% fiber volume content

(b) 0.4% fiber volume content

(c) Limit of Proportionality [*LOP*] in T12

Fig. 11. Initial part of load–deflection curve.

contents (0.4% and 1.2%) in an identical matrix. The four fiber types were high strength steel twisted (T-), high strength steel hooked (H-), high molecular weight polyethylene spectra (SP-), and PVA-fibers. All test series showed deflection-hardening behavior except specimens with 0.4% PVA-fibers, and very different performance levels were noted in terms of load carrying capacity (equivalent bending strength), energy absorption capacity (toughness), and cracking behavior (number of cracks), as a function of fiber type and volume content. The following observations and conclusions can be made based on the limited experimental study conducted.

- Deflection-hardening FRCC behavior can be obtained for low volume fractions (0.4%) of T-, SP-, and H-fibers.
- T-fiber specimens showed the highest load carrying capacity or MOR at 1.2% fiber volume contents, that is, 13.08 MPa. The order of performance in terms of equivalent bending strength, f_{MOR}, is observed to be as follows: T-fibers > H-fibers > SP-fibers > PVA-fibers.
- At large deflections of $\delta_{L/150}$ and $\delta_{L/100}$, T-fiber specimens exhibited the highest energy absorption capacity. The order of performance at this deflection level is as follows: T-fibers > H-fibers > SP-fibers > PVA-fibers.
- Spectra (SP-) fibers generated the highest deflection capacity at maximum resistance, δ_{MOR}.
- Although all fibers (T-, H-, SP-, and PVA-fiber) showed multiple cracking during deflection-hardening response when used at 1.2% fiber volume fraction, significantly different cracking behavior was observed. T- and SP-fiber specimens generated many cracks while PVA specimens generated only 2–3 cracks, and H-fiber specimens showed an intermediate number of cracks. The order of performance in terms of cracking behavior is as follows: T-fibers > SP-fibers > H-fiber > PVA-fibers.
- Comparison between the test program with a lower strength matrix and another test program with a higher strength matrix shows that increasing the matrix compressive strength increases the performance of T-fiber specimens significantly more than that of H-fiber specimens. In other words, T-fibers are able to take better advantage of a higher strength matrix than H-fibers.

The test results were used to critique the new ASTM Standard C 1609/C 1609M-05 [3]. In particular, it was noted that there are difficulties in applying the new standard to deflection-hardening materials. Two suggestions were made:

- Computations of toughness should be extended to $L/100$ and even $L/50$ if the case justifies it.
- A first peak point cannot always be found in the initial portion of a load–deflection curve, especially if the specimen shows stable deflection-hardening response. Therefore, the LOP as defined in the previous standard (ASTM Standard C 1018-97 [7]) is more generally applicable and should be used instead.

Acknowledgments

The research described herein was sponsored by the National Science Foundation under Grant Nos. CMS 0408623, 0530383, and 0754505. The opinions expressed in this paper are those of the authors and do not necessarily reflect the views of the sponsor.

References

[1] Naaman AE. Toughness, ductility surface energy and deflection-hardening FRC composites. In: Proceedings of JCI workshop on ductile fiber reinforced cementitious composites (DFRCC) – application and evaluation, Japan Concrete Institute, Tokyo, Japan, October 2002. p. 33–57.
[2] Soranakom C, Mobasher B. Correlation of tensile and flexural responses of strain softening and strain hardening cement composites. Cement Concrete Compos 2008;30(6):465–77.
[3] ASTM C 1609/C 1690M-05. Standard test method for flexural performance of fiber reinforced concrete (using beam with third-point loading). American Society of Testing and Materials, January 2006. p. 1–8.
[4] Soroushian P, Bayasi Z. Fiber-type effects on the performance of steel fiber reinforced concrete. ACI Mater J 1991;88(2):129–34.
[5] Gopalaratnam S, Shah SP, Batson GB, Criswell ME, Ramakrishnam V, Wecharatana M. Fracture toughness of fiber reinforced concrete. ACI Mater J 1991;88(4):339–53.
[6] Balaguru P, Narahari R, Patel M. Flexural toughness of steel fiber reinforced concrete. ACI Mater J 1992;89(6):541–6.
[7] ASTM C 1018-97. Standard test method for flexural toughness and first-crack strength of fiber reinforced concrete (using beam with third-point loading). American Society of Testing and Materials, October 1998. p. 544–51.
[8] Banthia N, Trottier J-F. Test methods for flexural toughness characterization of fiber reinforced concrete: some concerns and a proposition. ACI Mater J 1995;92(1):1–10.
[9] Chandrangsu K, Naaman AE. Comparison of tensile and bending response of three high performance fiber reinforced cement composites. In: Naaman AE, Reinhardt HW, editors. Proceeding pro 030: high performance fiber-reinforced cement composites (HPFRCC4), RILEM Publications, June 2003. p. 259–74.
[10] Naaman AE, Reinhardt HW. Proposed classification of FRC composites based on their tensile response. Mater Struct 2006;39(5):547–55.
[11] Ozyurt N, Mason TO, Shah SP. Correlation of fiber dispersion, rheology and mechanical performance of FRCs. Cement Concrete Compos 2007;29(2):70–9.
[12] Kim D. Strain rate effect on high performance fiber reinforced cementitious composites. Ph.D. thesis, University of Michigan, Ann Arbor; 2008.